Title

Controls on carbon storage and weathering in volcanic soils across a high-elevation climate gradient on Mauna Kea, Hawaii

Journal

Ecology, 97(9)

ISSN

0012-9658

Authors

Kramer, Marc G
Chadwick, Oliver A

Publication Date

2016-09-01

DOI

10.1002/ecy.1467

Peer reviewed

Ecology, 97(9), 2016, pp. 2384–2395

Controls on carbon storage and weathering in volcanic soils across a high-elevation climate gradient on Mauna Kea, Hawaii

Marc G. Kramer[1,3] and Oliver A. Chadwick[2]

[1]*School of the Environment, Washington State University, Vancouver, Washington 98686 USA*
[2]*Department of Geography, University of California, Santa Barbara, California 93106 USA*

Abstract. Volcanic ash soils retain the largest and most persistent soil carbon pools of any ecosystem. However, the mechanisms governing soil carbon accumulation and weathering during initial phases of ecosystem development are not well understood. We examined soil organic matter dynamics and soil development across a high-altitude (3,560–3,030 m) 20-kyr climate gradient on Mauna Kea in Hawaii. Four elevation sites were selected (~250–500 mm rainfall), which range from sparsely vegetated to sites that contain a mix of shrubs and grasses. At each site, two or three pits were dug and major diagnostic horizons down to bedrock (intact lava) were sampled. Soils were analyzed for particle size, organic C and N, soil pH, exchangeable cations, base saturation, NaF pH, phosphorous sorption, and major elements. Mass loss and pedogenic metal accumulation (hydroxlamine Fe, Al, and Si extractions) were used to measure extent of weathering, leaching, changes in soil mineralogy and carbon accumulation. Reactive-phase (SRO) minerals show a general trend of increasing abundance with increasing rainfall. However carbon accumulation patterns across the climate gradient are largely decoupled from these trends. The results suggest that after 20 kyr, pedogenic processes have altered the nature and composition of the volcanic ash such that it is capable of retaining soil C even where organic acid influences from plant material and leaching from rainfall are severely limited. Carbon storage comparisons with lower-elevation soils on Mauna Kea and other moist mesic (2,500 mm rainfall) sites on Hawaii suggest that these soils have reached only between 1% and 15% of their capacity to retain carbon. Our results suggest that, after 20 kyr in low rainfall and a cold climate, weathering was decoupled from soil carbon accumulation patterns and the associated influence of vegetation on soil development. Overall, we conclude that the rate of carbon supply to the subsoil (driven by coupling of rainfall above ground plant production) is a governing factor of forms and amount of soil organic matter accumulation, while soil mineralogy remained relatively uniform.

Key words: carbon storage; ecosystem development; short-range-ordered minerals; soil formation; soil organic carbon; volcanic ash; weathering.

Introduction

Volcanic soils occupy only 0.8% of the global land area but store as much as 5% of the global soil carbon (C) pool (Dahlgren et al. 2004). These soils have unique characteristics that make them particularly useful for probing chemical processes responsible for stabilizing organic matter during ecosystem development (Vitousek et al. 1997). Short-range-ordered (SRO) minerals accumulate in soils as primary volcanic minerals weather (Dahlgren et al. 2004) and they are associated with storage of large amounts of C (Vitousek et al. 1997, Kramer et al. 2012). There are strong feedbacks between the accumulation of organic acids in soil and weathering intensity. Carbon inputs (through net primary productivity and rainfall) influence both mineral weathering rates (Berner 1992, Drever 1994, Cochran and Berner 1996), and the carbon compounds available to react with secondary minerals (Kaiser and Guggenberger 2000). However, the extent to which vegetation inputs are responsible for the concomitant formation of reactive minerals in soils through weathering and for providing a supply of carbon to those minerals for C storage is not fully understood.

Chronosequence (Long Substrate Age Gradient [LSAG]) studies in mesic environments across the Hawaiian Islands identify three distinct phases of mineral–carbon interactions (Vitousek et al. 1997, Torn et al. 1997, Chorover et al. 2004): (1) During early stages of soil development (10^2–10^3 yr) primary minerals and soil organic matter (SOM) are mostly chemically distinct with chemical bonding occurring where SRO minerals are forming along mineral edges. Here the turnover time of carbon compounds is relatively short. (2) There follows a relatively long period (10^3–10^5 yr) when most primary minerals have transformed to hydrated and chemically reactive SRO minerals, which are strongly interbonded with SOM forming a three-dimensional heterogeneous gel. Here the turnover time of SOM is long (>20 kyr). (3) Finally there is an extended period (10^5–10^7 yr) where SRO minerals have reorganized into crystalline

Manuscript received 12 August 2015; revised 9 February 2016; accepted 4 March 2016; final version received 3 May 2016. Corresponding Editor: J. B. Yavitt.
[3]E-mail: marc.kramer@wsu.edu

secondary minerals that sorb SOM to their surfaces but do not have it incorporated into the mineral matrix. Here the turnover time of SOM is again relatively short because SOM is no longer protected within the gel. Understandably, most of the mineral–carbon interaction research associated with these chronosequences has focused on the second stage of ecosystem development where B horizons can contain as much as 70% SRO mineral and store 10% C (Kramer et al. 2012). The principal source for this C is dissolved aromatic acids derived from dense forest vegetation via organic horizons. These aromatic acids were retained via hydroxyl (OH^-) functional groups prevalent in the SRO minerals (Kramer et al 2012). We know much less about alteration mechanisms that occur during stage 1 ecosystem development that can be greatly extended in time under drier and colder climates, where both weathering and carbon inputs are limited.

A central goal in this study was to better understand carbon storage and soil development processes that occur during the initial phase of cinder weathering and ecosystem development in the cold, dry environments that exist near the summit of Mauna Kea. We report on the formation of SRO minerals during early (stage 1) weathering of volcanic ejecta and accumulation of SOM at four sites along a 500-m transect running from near the top of Mauna Kea downwards to the contact of the mountain with the atmospheric inversion layer. Although formed in the same ~20 kyr ejecta, the top three sites support little vegetation due to low rainfall and low temperature whereas the lowest-elevation site supports a relatively robust growth of shrubs and grasses. Our objectives were to (1) evaluate the state of weathering and amount SRO mineral formation, (2) quantify carbon storage and it's relationship to SRO minerals, and (3) put these results in the broader context of mineral–SOM reactions and soil carbon storage for volcanic soils in Hawaii and elsewhere.

Site description

We sampled soils across a high-altitude (3,560–3,030 m), 20-kyr, elevation gradient on Mauna Kea in Hawaii (Fig. 1A, B) 19.8207° N, 155.4681° W. Four sites selected along the climate gradient range from arid-periglacial at the top two 3,560- and 3,440-m sites, with sparse grass vegetation to inversion-layer influenced at the bottom two (3,260–3,030 m) sites. Rainfall amounts were estimated to range ~250–300 and 400–500 mm by using elevation-base interpolation from rainfall maps of Hawaii (Giambelluca et al. 2013). Given that the bottom two sites are influenced by the inversion layer, our rainfall estimates and the interpolation methods are considered coarse approximations.

Materials and Methods

Soil profiles were sampled down to intact (consolidated) material (~0.5–1 m depth). The soils are formed in an aerially extensive covering of volcanic ejecta that formed during late-stage alkalic eruptions. The deposits are assigned an age of ~20 kyr in part because they have been disrupted by the most recent glacial moraines near the top of the mountain (Wolf and Morris 1996). The soils formed on hawaiite (Laupahoehoe) lava and cinders, but vary with climate (mean annual temperature = 0–3°C, mean annual precipitation ≈ 250–500 mm; Raine 1939, Woodcock et al. 1966, Woodcock 1974; Fig. 1A, B). The vegetation on these surfaces range from sparse grass on the upper two elevation sites, to grass and shrub (*Māmane Sophora chrysophila* ʻĀheahea [*Chenopodium oahuense*]) at the lower two sites. Common grasses include two native grasses, alpine hairgrass (*Deschampsia nubigena*) and pili uka (*Trisetum glomeratum;* Hartt and Neal 1940).

Soil sampling

All soils formed from volcanic ash and cinders. All soil sampling sites have a south-southwest aspect and are situated on comparable geomorphic landscape positions on flat slopes ranging from 1% to 5%. There was no evidence of accelerated erosion at any of the sampling sites. At all field sites, soils were sampled by genetic horizon to weathered rock or to about 1 m in depth.

The soils from the two highest-elevation sites are similar to the soils of the high mountain deserts and to the soils of cold deserts with periglacial and aeolian processes evident (Raine 1939, Woodcock et al. 1974, Ugolini 1974, 1975). Soil classifications for each of the four sites ranged from cinder land (an undeveloped mixture of fine cinders, pumice, and volcanic ash) 3,440 and 3,560 m to Ashy-skeletal over fragmental or cindery, amorphic over mixed, isomesic Humic Ustivitrands at 3,260 and 3,030 m sites (Fig. 2A–D) (Soil Conservation Service 1973). Samples from each of the organic and mineral horizons were collected using standard U.S. Soil Survey diagnostic criteria (Schoeneberger et al. 1998). Air-dried samples were sieved (2-mm mesh) to remove large organic and mineral particles. A 1-mm sieve was used to further pick out large organic particles including roots, bark, and other identifiable plant parts.

Soil chemical and physical characterization

Soil chemical and physical characterization was completed on moist or air-dried samples using the following standard procedures (Burt 2004): particle size was determined by suspending a 20-g air dried sample on a shaker for 2 h with 45 mL 3% hexametaphosphate as a dispersant, wet sieving the sand fraction and using 90-min settling time to separate the silt and clay fraction (Kettler et al. 2001); extractable bases by NH_4OAC buffered at pH 7; extractable acidity by $BaCl_2$-tri-ethanolamine IV buffered at pH 8.2 and back titration with HCl; extractable Al by 1 N KCl; CEC by NH_4OAC buffered at pH 7 and by sum of bases plus Al; Al saturation by

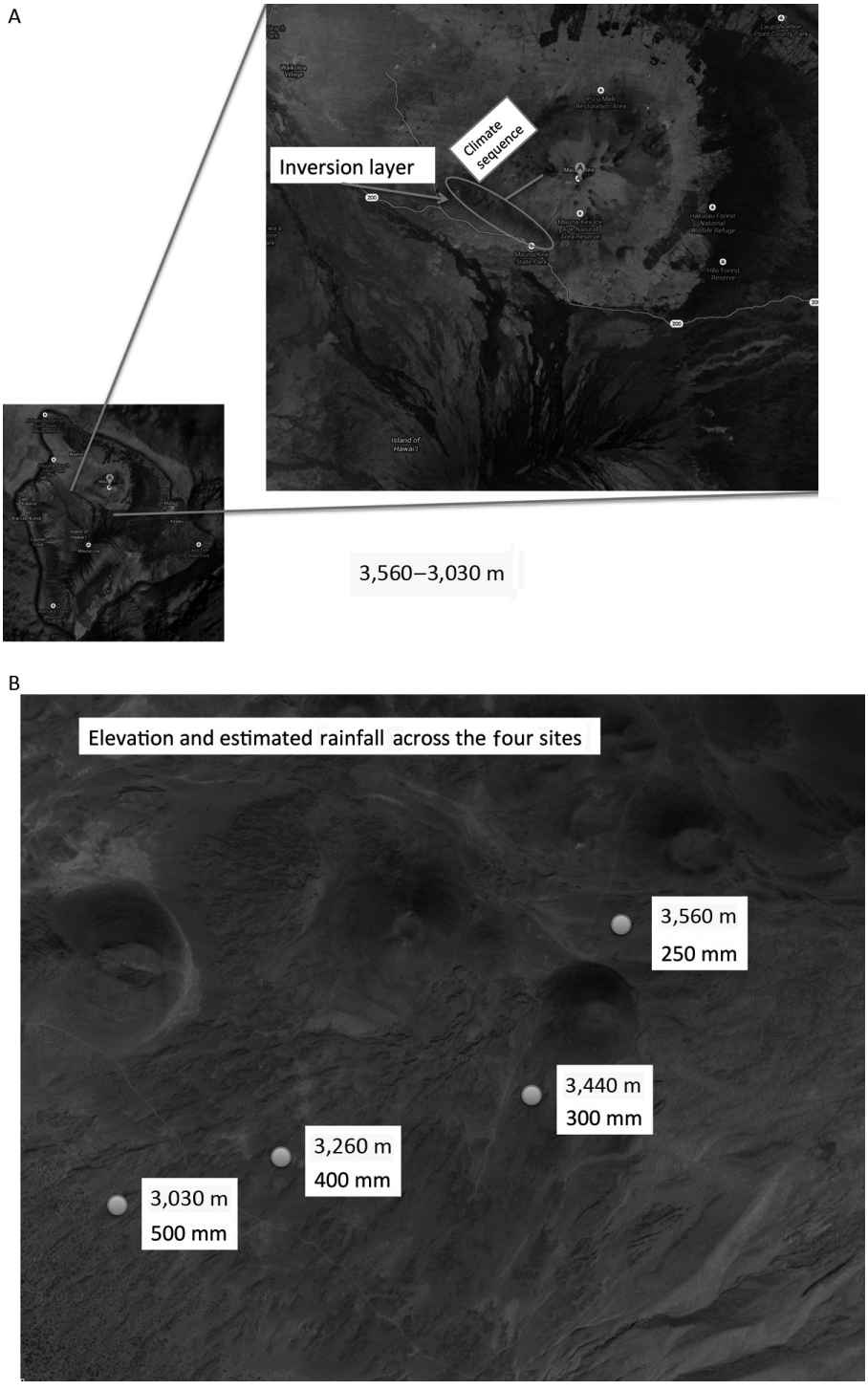

FIG. 1. (A) Vicinity map of the Mauna Kea climate gradient used in this study on the island of Hawai'i. (B) Location, elevations, and rainfall of the four sites used in the Mauna Kea climate gradient.

bases plus Al; base saturation by NH_4OAC buffered at pH 7; pH in 1:1 soil–water mixture; bulk density was estimated using standard coring techniques (Burt 2004); and total elemental analysis of the fine-earth (< 2 mm) fraction of the soil was made by X-ray fluorescence on a borate fusion for all elements. Mass fraction lost or gained, $\tau_{j,s}$, for each element was calculated as (Bern et al. 2015):

$$\tau_{j,s} = \left(\frac{C_{j,s}}{C_{j,p}} \times \frac{C_{i,p}}{C_{i,s}} \right) - 1$$

where C_j is the concentration of an element of interest (j) and an index component (C_i) is the concentration of an element assumed to be immobile. Each element is measured for the parent material (p) and soil (s). NaF pH was determined using a 1-g sample is mixed with 50 mL of 1 mol/L NaF and stirred for 2 min. While the sample is being stirred, the pH was read at exactly 2 min in the upper one-third of the suspension. P sorption was measuring using a 5-g soil sample, shaken in a 25-mL aliquot of a 1,000 mg/L P solution for 24 h. The mixture was centrifuged at 2,000 rpm for 15 min. Phosphorous was concentration was measured using inductively coupled plasma (ICP).The New Zealand P retention (Blakemore et al. 1987) was determined the initial P concentration minus the P remaining in the sample solution and is reported as percentage of P retained.

Quantification of short-range-order minerals

SRO minerals were quantified using hydroxylamine. The soil was extracted using 0.275 mol/L sodium hydroxlamine, pH 3.25, 1:100 soil:extractant (Burt 2004). Hydroxlamine selectively removes short-range-ordered hydrous oxides of Fe and Al such as allophane and ferrihydrite, but is a poor extractant of imogolite and layer silicates and does not extract crystalline hydrous oxides of Fe and Al, opal, or crystalline silicate (Wada 1989). Most commonly Fe, Al, and Si in the supernatant are measured as an indicator of SRO mineral quantity, but in this case, the mass of SRO mineral was also determined by recording weight loss after extraction (Vitousek et al. 1997, Chadwick et al. 2003). Hydroxlamine-extractable organic carbon released into solution during SRO mineral dissolution was determined (using the same approach as Kramer et al. 2012); by measuring dissolved organic carbon (DOC) in solution and then subtracting out the background hydrloxlamine C concentration. Carbon and SRO mineral dissolution and release in deionized water was used as a control.

Carbon and nitrogen analyses

Carbon and nitrogen were measured with a coupled continuous-flow elemental-analyzer–isotope-ratio mass spectrometer (EA-IRMS) system with a Carlo-Erba model 1108 EA (CE Elantch, Lakewood, New Jersey, USA) interfaced to a Thermo-Finnigan Delta Plus XP IRMS (Thermo Fisher Scientific, Walton, Massachusetts, USA). Dry samples (<2 mm) were ground finely with a zirconium mortar and pestle and loaded into tin boats. One standard was run for every 10 unknowns, and two blanks and conditioning and calibration standards were included at the beginning and end of each run. Samples were run in duplicate and were always within the range of the standards. Analysis of internal standards indicated an analytical error of <5% for N and <2% for C. Samples were analysed at the light stable isotope facility of the University of California, Santa Cruz.

Comparison with Hawaii LSAG sites and xeric sites elsewhere

We compared the amount of DOC contained within the SRO minerals across the high-elevation Mauna Kea climate gradient with lower-elevation, moist-mesic, long substrate age gradient (LSAG; 2,500 mm rainfall) sites across Hawaii. We also compared the bulk soil C concentration observed relative to SRO mineral content with the 2,500-mm rainfall LSAG sites and a xeric (1,000-mm rainfall) site on Mount Shasta (Takahashi et al. 1993, Kramer et al. 2012).

Using results from Longathan and Swindale (1969) as well as Kramer et al. (2012), we extended the range of our high-elevation climate sequence from the 250–500 mm rainfall gradient by adding five additional lower-elevation sites, which increased in rainfall up to 2,500 mm on Mauna Kea. We evaluated carbon content in the deep subsoil relative to rainfall between ~250 mm rainfall up to 2,500 mm at nine elevation (and consequently rainfall) sites. We also plotted C/N ratio against rainfall across the entire (250–2,500 mm) climate sequence of Mauna Kea.

Results

Soils at the highest three elevation sites (~250–400 mm rainfall) lacked an organic soil horizon and instead were dominated by surface pebbles and stones characteristic of desert pavement (Fig. 2A), which varied in thickness from 8 to 20 cm. This was underlain by brown yellowish coarse-grained (sand-sized) tephra (dust) and cinder beneath (Fig. 2B). By contrast, the wettest (~500 mm RF), lowest-elevation site contained an abundance of overstory shrubs and understory grasses (Fig. 2C), and had an organic soil horizon underlain by an A horizon and fine-grained tephra (a Bw/tephra horizon follows a C [cinder] horizon; Fig. 2D). Clay content across all the sites and all depths was low (<7%) and ranged from 1.6% ± 0.6% (mean ± SE) at the highest elevation (~250 mm RF), increasing slightly at the lowest elevation (~500 mm RF) site to 6.6% ± 0.3% in the Bw horizon. Silt content increased in the A and Bw/fine tephra horizon of the two lower-elevation wetter (~400–500 mm RF) sites to 20.5% ± 1.2% but ranged between 5.6% ± 0.9% and 8.3% ± 4.6% in the coarse tephra horizons of the highest-elevation sites (~250–300 mm RF) and in all the cinder soil horizons.

Extractable Al + 1/2 Fe hydroxylamine content was lowest at the highest-elevation (~250 mm RF) site (between 2.57% ± 0.51% and 3.81% ± 0.63%) and increased with decreasing elevation and increasing rainfall up to 5.86% ± 0.97% and 5.93% ± 1.35%) at the lowest-elevation (~500 mm RF) site. Carbon content was extremely low (<0.18%) at the highest-elevation (~250 mm RF) site

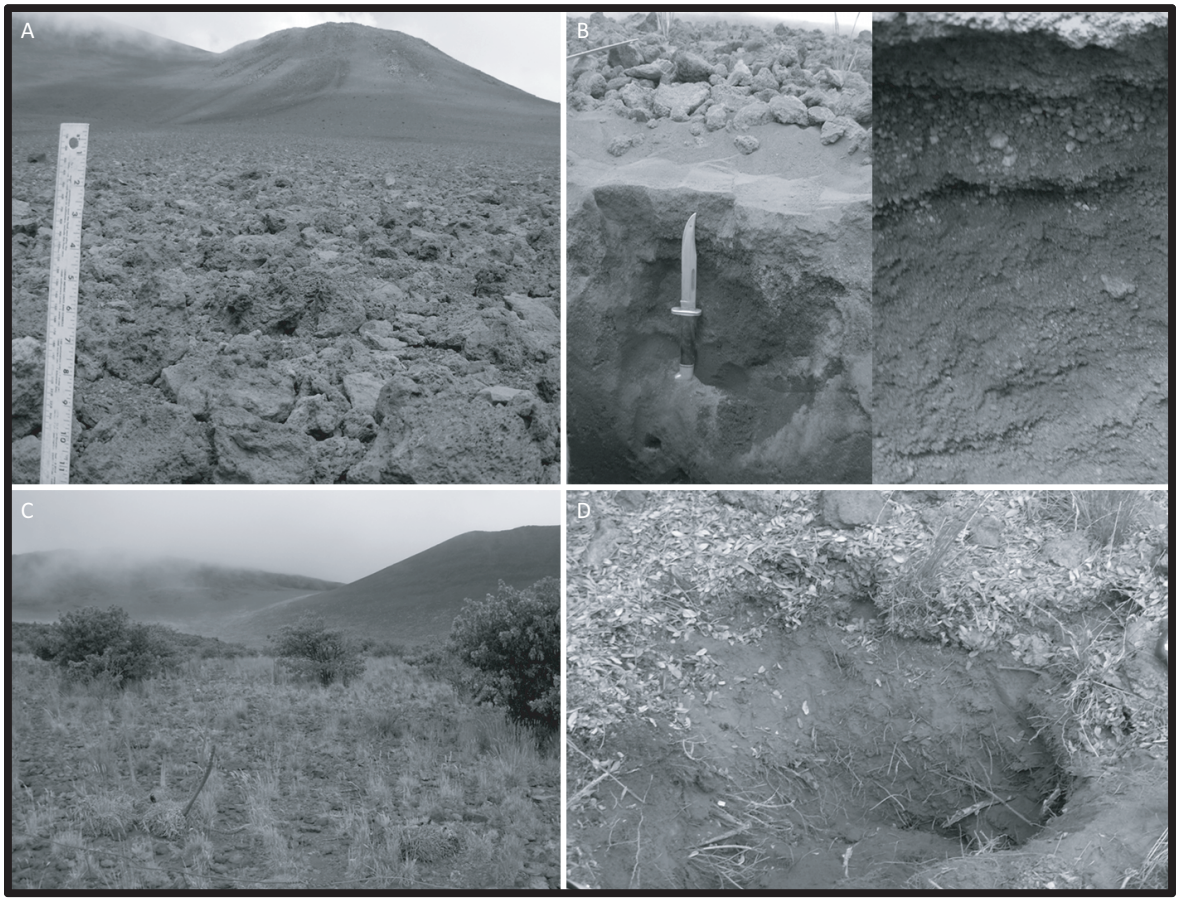

FIG. 2. (A) Sparse vegetation and desert pavement features of the highest-elevation (3,563m) site. (B) Aeolian dust beneath desert pavement at the highest-elevation sites underlain by sand grained cinder particles. (C) Overstory vegetation (māmane shrubs) and grasses occurring in abundance at the lowest-elevation site. (D) Major diagnostic soil horizons (Oiea, A, and Bw) soil horizon formation at the lowest (3,031 m) elevation site.

across all soil horizons and increased with lower elevations to up to 2.17% ± 0.46% and 2.82% ± 0.49%) in the A and Bw horizon of the lowest-elevation (~500 mm RF) site. Carbon content was low (<0.38%) across all sites in the cinder horizon and showed no consistent change or trend across elevation/rainfall (Fig. 3A, Table 1). C/N ratio increased with decreasing elevation and increasing rainfall from 7.9 ± 0.2 up to 14.3 ± 0.3 (Table 1). Cation exchange capacity was lowest at the highest elevation (~250 mm RF) site (<17 ± 4.0 mEq/100 g) and increased up to 41.68 ± 6.38 in the Bw horizon of the lowest elevation (~500 mm RF) site with no trend in the cinder layer observed across sites. Base saturation was lowest at the highest-elevation (~250 mm RF) site (15.51 ± 3.3 and 23.46 ± 15.81) and increased to 35.41 ± 4.41 at the lowest-elevation (~500 mm RF) site. Soil pH showed a slight overall trend of decline from 7 ± 0.1 to 6.4 ± 0.1 with decreasing elevation and increasing rainfall. All the results are summarized by depth and site in Table 1.

Carbon accumulation with depth across sites are shown in Fig. 3A, B. Overall the depth profiles show a trend of increasing C concentration with decreasing elevation and increasing rainfall. The two highest-elevation (~250–300 mm rainfall) sites are uniformly low in C content with depth. The lowest-elevation (~500 mm rainfall) sites show a pronounced increase in C content in the A and B horizons followed by a strong decline in the cinder horizon (Fig. 3A). Total C stocks across sites increased from 3.1 ± 1.5 up to 118.9 ± 42.5 Mg C/ha under the māmane shrubs of the lowest-elevation (~500 mm rainfall) site and is shown in Fig. 3B.

Little loss of major elements was observed with decreasing elevation and increasing rainfall (Table 2). Depth trends of Si depletion (Fig. 4) indicate slightly increasing Si loss with decreasing elevation and increasing rainfall with a significant depletion pattern observed in the A and Bw horizons of the lowest-elevation (~500 mm site) site (Fig. 4). NaF pH and P sorption increased significantly with increasing SRO content across the elevation gradient (as measured by Alh + 1/2 Feh; Fig. 5A, B).

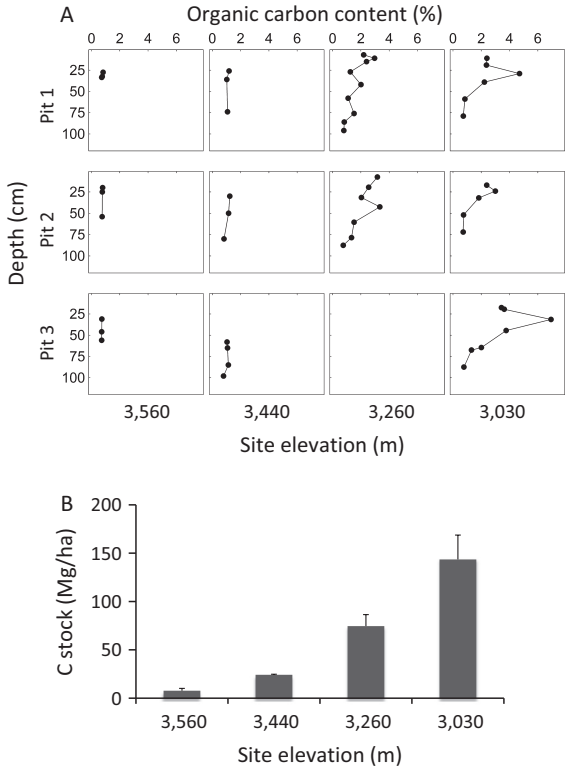

FIG. 3. (A) Soil depth profiles of organic carbon content at each of the soil pits collected across the climate sequence on Mauna Kea. (B) Carbon stocks (mean and SE) at each of the high-elevation sites on Mauna Kea.

Carbon content of the cinder layer did not change significantly across the elevation/rainfall gradient, while SRO mineral content (as measured by Alh + 1/2 Feh) did (Table 1, Fig. 6). The amount of C retained by SRO minerals is shown in Fig. 7A. The data from all the Mauna Kea pits are plotted along with sites from the moist (2,500 mm rainfall), mesic LSAG sites, which retained significantly higher amounts of C in the SRO minerals than those on Mauna Kea. The relationship between bulk C content and SRO content (measured by Alh + 1/2 Feh) is shown in Fig. 7B, which also shows C content SRO relationships for wetter lower-elevation (2,500 mm) udic rainfall sites and an additional xeric site from Mount Shasta. The soil C concentration observed relative to SRO mineral content was much lower than either moist mesic (2,500 mm) rainfall LSAG sites across Hawaii or a xeric (1,000 mm) site in Mount Shasta (Fig. 7B). The results indicate that carbon contents relative to SRO mineral content decreases with decreasing rainfall and reaches a near minimum near the summit of Mauna Kea. Using results from Longathan and Swindale (1963) as well as Kramer et al. 2012) carbon content in the deep subsoil relative to rainfall was found to increase with increasing rainfall reaching a maximum of 10% around 1,500 mm rainfall (Fig. 8A). C/N ratio from was found to increase consistently from 8 at ~250 mm RF up to 32 at the wettest (2,500 mm) rainfall site (Fig. 8B).

DISCUSSION

Weathering across the climate gradient on Mauna Kea

Weathering at the highest-elevation (3,560 m) site advanced largely in the absence of any influence from vegetation and was due principally to periglacial processes and the limited (~250 mm MAP) rainfall occurring in a cool climate. Little evidence for redistribution or elemental loss of Si, Al, or Fe was found and clay content was extremely low indicating very low secondary clay formation during the weathering process (<3%; Tables 1 and 2, Fig. 4). Most of the tephra and cinder consisted of sand-sized particles, suggesting little congruent dissolution weathering occurred. However, significant (20–30% by mass) alteration of the volcanic ash into amorphous minerals after 20 kyr (Table 1) was found. The amount of free Fe, Al, and Si oxides (as measured by selective extraction using hydroxylamine) are similar to those reported by Ugolini (1975) who sampled soils in the 3,500-m elevation area to a shallower depth of 35 cm. The SRO content observed at this site is comparable to youngest (300 yr) LSAG site (Kramer et al. 2012). Weathering at the 3,440-m elevation site (~300 mm rainfall) increased with both a slight increase in clay content (1–2%) and an 84% increase in SRO mineral content (nearly doubling), while rainfall was estimated to only increase by approximately 25%. As with the 3,560-m-elevation site however, evidence for solute loss or pedogenic redistribution of metals throughout the soil profile was limited (Table 2, Fig. 4). Vegetation was very limited at the site, however, an extremely sparse distribution of several species of grass was observed. Evidence for the predominance of periglacial and aeolian processes was prevalent with pebble (and larger-sized) stones composing a pavement that formed the first soil horizon

At the 3,260-m-elevation site (~400 mm rainfall), the influence of vegetation on weathering was more apparent with a very sparse distribution of mamane shrubs and relatively extensive native grass cover. Short-range-ordered mineral content in the cinder layer was double that of the highest-elevation driest (~250 mm rainfall) site (Table 1). While higher carbon was found in the upper tephra (A and Bw soil horizon), carbon content was only 0.31% in the cinder horizon, suggesting that weathering was still decoupled from carbon inputs from the plants (Table 1). Silicon depletion, and an increase in silt content (with a concomitant decline in sand content) although slight, was evident at the site and increased with soil depth indicating some solute loss occurred during weathering, which was also more congruent than the higher-elevation sites (Table 1, Fig. 4).

Weathering was greatest at the lowest 3,030-m-elevation site (~500 mm rainfall), with māmane shrubs and native grass covering much of the area (Fig. 1C). SRO mineral content in the cinder layer was higher than any of the other sites (Table 1). While higher carbon content (>2%) was found in the upper tephra (A and Bw soil horizon), carbon

Table 1. Selected soil properties from sites sampled across the elevation climate gradient on Mauna Kea.

Site elevation (m)	Estimated rainfall (mm)	Soil horizon	Profile depth (cm)	Soil fraction (%)								CEC (mEq/100 g)	Base saturation (%)	pH
				<2 mm	Sand	Silt	Clay	Alh + 1/2 Feh	C	N	C/N			
3,560	250	surface pebbles	0–10	7.8 (4.1)	–	–	–	–	–	–	–	–	–	–
3,560	250	coarse-grained tephra	10–23	76.7 (5.2)	90.1 (5.2)	8.3 (4.6)	1.6 (0.6)	3.81 (0.51)	0.18 (0.01)	0.02 (0.01)	7.9 (0.3)	16.66 (3.68)	15.51 (3.53)	6.8 (0.1)
3,560	250	C, cinder	23–59	59.3 (4.2)	97.1 (0.7)	2.0 (0.5)	1.0 (0.2)	2.57 (0.63)	0.05 (0.01)	0.00 (0.00)	7.9 (2.2)	12.98 (3.91)	23.46 (15.81)	7.0 (0.1)
3,440	300	surface pebbles	0–20	2.1 (0.2)	–	–	–	–	–	–	–	–	–	–
3,440	300	coarse-grained tephra	20–35	84.2 (2.9)	92.3 (0.9)	5.6 (0.9)	2.2 (0.3)	3.33 (0.38)	0.38 (0.08)	0.04 (0.01)	9.5 (0.5)	14.58 (1.01)	8.82 (2.29)	6.5 (0.1)
3,440	300	cinder	35–97	75.5 (9.1)	90.8 (1.4)	5.9 (0.7)	3.4 (1.0)	4.26 (0.31)	0.37 (0.03)	0.03 (0.01)	11.3 (0.3)	18.92 (2.64)	21.91 (4.22)	6.7 (0.1)
3,260	400	surface pebbles	0–8	–	–	–	–	–	–	–	–	–	–	–
3,260	400	A, fine tephra	8–18	90.6 (—)	78.2 (—)	17.5 (—)	4.2 (—)	3.02 (—)	2.49 (—)	0.25 (—)	9.9 (—)	24.99 (—)	26.54 (—)	6.3 (—)
3,260	400	Bw, fine tephra	18–77	85.1 (—)	77.7 (—)	19.4 (—)	2.9 (—)	4.32 (—)	1.32 (—)	0.13 (—)	10.1 (—)	30.13 (—)	23.14 (—)	6.7 (—)
3,260	400	C, cinder	77–100	90.7 (—)	90.3 (—)	6.6 (—)	3.1 (—)	5.14 (—)	0.31 (—)	0.03 (—)	12.7 (—)	22.29 (—)	33.48 (—)	6.9 (—)
3,030	500	Oiea	0–7	–	–	–	–	–	39.54 (3.54)	2.09 (0.25)	18.9 (0.7)	–	–	–
3,030	500	A, fine tephra	7–20	96.9 (1.3)	82.5 (1.2)	13.5 (0.5)	3.9 (0.7)	4.71 (1.12)	2.17 (0.46)	0.21 (0.04)	10.5 (0.2)	22.74 (1.21)	34.37 (4.58)	6.4 (0.1)
3,030	500	Bw, fine tephra	20–47	94.7 (2.2)	72.9 (1.5)	20.5 (1.2)	6.6 (0.3)	5.96 (0.97)	2.82 (0.49)	0.25 (0.04)	11.5 (0.2)	41.68 (6.32)	16.66 (4.69)	6.5 (0.1)
3,030	500	C, cinder	47–81	91.1 (3.5)	95.4 (1.1)	2.6 (0.3)	2.1 (0.8)	5.83 (1.35)	0.11 (0.03)	0.01 (0.01)	14.3 (0.3)	16.01 (0.61)	35.41 (4.41)	6.8 (0.1)

Notes: Properties include elevation, rainfall, <2 mm fraction, sand, silt, clay content (%), %C, %N, C/N, extractable Al + 1/2 Fe hydroxylamine content (Alh + 1/2 Feh; %), base saturation (%), cation exchange capacity, and soil pH (measured in a 1:1 mixture of soil and water) All values are reported as means, with SE in parentheses.

content was only 0.11% in the cinder horizon, suggesting that even in the highest rainfall site, weathering was still decoupled from carbon inputs from the plants in the deeper cinder. The degree of alteration was high. Significant silicon depletion was observed in distinct soil horizons (A and Bw; Fig. 4) and a strong increase in silt content (with a concomitant decline in sand content) were found at the lowest-elevation sites with the most rainfall (Table 1). Weathering in the A and Bw mineral soil were strongly influenced by plant matter, with both a prevalence of discernable root fragments and in notable increase in silt and clay content in those horizons.

Overall increased chemical weathering was observed across the climate gradient and the degree of weathering was largely decoupled from the influence of vegetation. Increasing rainfall amounts resulted predominantly in increased accumulation SRO minerals throughout the depth profile and only a slight increase in clay content or soil carbon accumulation. The lower two-elevation sites contained thick A and Bw horizons above the cinder layer, which had a noticeably higher silt, clay and carbon content. These A and Bw soil horizons showed evidence of elemental Si loss at the lower-elevation site, suggesting both the higher rainfall (~400–500 mm rainfall) and plants were responsible for more congruent weathering and formation of secondary mineral clays in the upper soil horizons.

Elsewhere in Hawaii, lower-elevation, warmer sites that receive 500 mm rainfall are subject to greater wet-dry fluctuations, less soil water flux due to greater evaporation rates, and consequently favor accumulation of crystalline minerals and greater accumulation of solutes (e.g., pedogenic carbonates; Chadwick et al. 2003, Ziegler et al. 2003). The high-elevation sites on Mauna Kea favor the persistence of SRO minerals, in spite of low rainfall amounts and we found little evidence for solute accumulation in any of the sites.

Carbon delivery, storage, and weathering

Kramer et al. (2012) concluded that high rates of dissolved organic production coupled with abundant

TABLE 2. Major elements with depth from sites sampled across the elevation climate gradient on Mauna Kea, including elevation, rainfall, including Alh, Feh, Sih (%), and major elements.

				Soil fraction (%)											
Elevation (m)	Rainfall (mm)	Soil horizon	Profile depth (cm)	SiO_2	Al_2O_3	Fe_2O_3	CaO	MgO	Na_2O	K_2O	TiO_2	MnO	P_2O_5	BaO	LOI
3,560	250	surface pebbles	0–10	48.81 (0.39)	18.14 (0.17)	11.82 (0.15)	6.27 (0.02)	3.71 (0.03)	4.11 (0.04)	1.64 (0.06)	2.79 (0.05)	0.23	0.96 (0.02)	0.07	1.26 (0.18)
3,560	250	fine-grained tephra	10–23	44.05 (0.71)	19.37 (0.26)	13.14 (0.14)	5.62 (0.14)	4.05 (0.09)	3.21 (0.11)	1.05 (0.07)	3.06 (0.04)	0.23	0.91 (0.02)	0.08	6.46 (1.05)
3,560	250	cinder	23–59	46.86 (0.91)	18.48 (0.39)	12.45 (0.13)	6.11 (0.13)	3.99 (0.08)	3.66 (0.16)	1.38 (0.12)	2.91 (0.06)	0.22	0.88 (0.01)	0.07	2.72 (0.81)
3,440	300	surface pebbles	0–20	50.77 (0.02)	18.67 (0.11)	9.97 (0.01)	5.77 (0.06)	3.12 (0.01)	4.5 (0.02)	1.85 (0.03)	2.28 (0.01)	0.22 (0)	0.97 (0.02)	0.08 (0)	1.56 (0.08)
3,440	300	fine-grained tephra	20–35	43.13 (0.44)	19.15 (0.06)	13.74 (0.08)	5.62 (0.05)	4.54 (0.08)	3.2 (0.06)	0.96 (0.03)	3.18 (0.01)	0.24 (0)	0.89 (0.01)	0.06 (0)	4.95 (0.46)
3,440	300	cinder	35–97	42.06 (0.22)	19.92 (0.08)	13.64 (0.03)	5.51 (0.03)	4.14 (0.05)	3.1 (0.04)	0.82 (0.03)	3.21 (0.02)	0.24 (0)	0.91 (0.01)	0.07 (0)	6.06 (0.22)
3,260	400	surface pebbles	0–8	50.12 (—)	17.73 (—)	10.47 (—)	6.26 (—)	3.51 (—)	4.21 (—)	1.66 (—)	2.51 (—)	0.21 (—)	0.95 (—)	0.08 (—)	1.46 (—)
3,260	400	A horizon (fine-grained tephra)	8–10	42.19 (—)	17.66 (—)	12.82 (—)	5.41 (—)	4.04 (—)	3.12 (—)	0.95 (—)	2.89 (—)	0.23 (—)	0.96 (—)	0.07 (—)	9.31 (—)
3,260	400	Bw and fine tephra	18–77	41.41 (—)	19.34 (—)	13.16 (—)	5.22 (—)	3.84 (—)	3.07 (—)	0.94 (—)	3.01 (—)	0.24 (—)	0.92 (—)	0.07 (—)	8.51 (—)
3,260	400	cinder	77–100	41.53 (—)	20.33 (—)	13.29 (—)	5.47 (—)	3.76 (—)	2.98 (—)	0.78 (—)	3.15 (—)	0.25 (—)	0.95 (—)	0.07 (—)	7.07 (—)
3,030	500	Oiea	0–7												
3,030	500	A horizon (fine-grained tephra)	7–20	43.04 (0.26)	17.45 (0.45)	13.12 (0.27)	5.64 (0.09)	4.35 (0.06)	3.24 (0.04)	1.04 (0.01)	2.94 (0.09)	0.24 (0)	0.85 (0.02)	0.07 (0)	7.71 (0.66)
3,030	500	Bw and fine tephra	20–47	35.54 (0.92)	20.49 (0.12)	14.06 (0.09)	4.62 (0.15)	4.11 (0.08)	2.38 (0.11)	0.68 (0.01)	3.28 (0.03)	0.25 (0)	0.91 (0.02)	0.05 (0)	13.47 (1.32)
3,030	500	cinder	47–81	43.28 (0.24)	19.54 (0.03)	13.24 (0.14)	5.93 (0.03)	4.09 (0.11)	3.26 (0.04)	0.93 (0.02)	3.08 (0.02)	0.24 (0)	0.89 (0.01)	0.07 (0)	5.15 (0.09)

Note: All values are reported as means with SE in parentheses.

SRO mineral formation were both critical factors in determining long-term C accumulation with SRO minerals. The NaF pH and P sorption results from Mauna Kea (Fig. 5A, B) indicate that the reactive mineral particles have amorphous mineral properties (hydroxlyated mineral surfaces with strong sorption potential; Fig. 5A, B) and are thus capable of retaining significant C stores. Although soil carbon accumulation increased across the climate gradient (Fig. 3B), the greatest increase occurred in the upper (A and Bw) soil horizons of the lower-elevation sites (Fig. 4), and little or no discernable increase in C storage was observed in the deeper cinder layers across the entire gradient in spite of the fact that the cinder became increasingly altered, with higher SRO content with increasing rainfall (Table 1, Fig. 6).

Carbon retention with SRO minerals in more moist mesic sites containing volcanic ash (2,500 mm rainfall) is considerably higher than the amount of carbon retained across this high-elevation climate gradient on Mauna Kea (Fig. 7A, B). Across more moist mesic (2,500 mm) rainfall sites, an excess of rainfall results in significant flux of DOC through the soil (Kramer et al. 2012). The lack of major elemental loss from any of the Mauna Kea sites suggests rainfall (<500 mm) is likely below a threshold at which throughflow ever occurs (Table 2, Fig. 4) indicating that rainfall mediated carbon delivery to the subsoil may be a limiting factor.

Using data from Longathan and Swindale (1963), we found that at a similar (20 kyr) age, rainfall and soil carbon content are higher at the lower-elevation deposits on Mauna Kea (Fig. 8A). Carbon accumulation increased

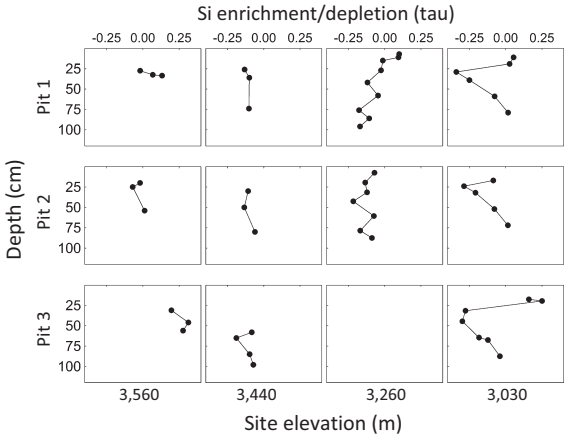

FIG. 4. Depth profiles of Si depletion and enrichment (tau) in soil pits from sites along the climate sequence on Mauna Kea.

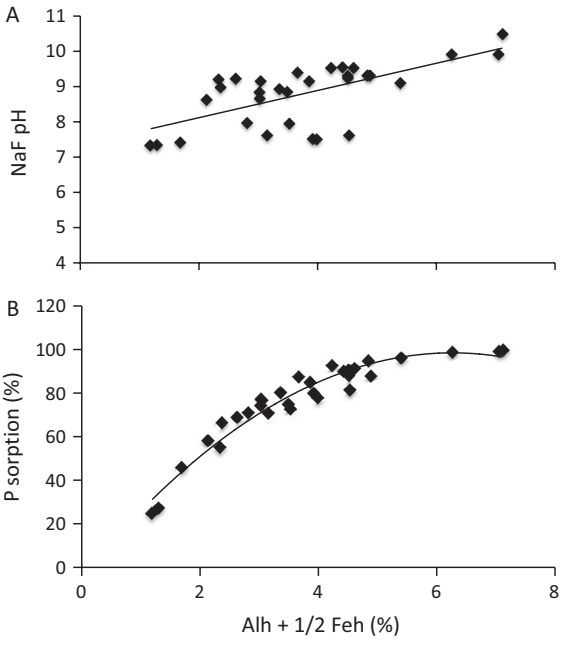

FIG. 5. (A) NaF pH characteristics in relation to short-range-ordered (SRO) mineral abundance (as measured by extractable Al + 1/2 Fe hydroxylamine content [Alh + 1/2 Feh]) from the soils across the climate sequence on Mauna Kea. (B) P sorption characteristics in relation to SRO mineral abundance (as measured by Alh + 1/2 Feh) from the soils across the climate sequence on Mauna Kea.

both at 660 mm and 1,170 mm and appears to have reached a soil C maximum at 1,530 mm rainfall of 9% in the B horizon, comparable to soil C concentrations at 2,500 mm rainfall (Kramer et al. 2012). Base saturation also declines at this rainfall to near zero (Longathan and Swindale 1963), corresponding to a climatically driven pedogenic threshold observed on other climate gradients studied in Hawaii (Chadwick and Chorover 2001, Chadwick et al. 2003). Thus, on the 20-kyr deposits, as rainfall increases from 1,500 mm to 2,500 mm, soil carbon storage by SRO minerals reaches a plateau (Fig. 8A).

We also compared our results to another Holocene (~20 kyr) volcanic ash site at 1,000 mm rainfall on Mount Shasta (Takahashi et al. 1993) to see if the data are consistent with our findings on Mauna Kea. While carbon concentrations relative to SRO content in the Mount Shasta site were greater than those found on high-elevation sites (<300 mm rainfall) of Mauna Kea, they were still considerably lower than the wetter (2,500 mm) mesic sites in Hawaii (Fig. 7B). Collectively, these results suggest that rainfall and vegetation drive carbon delivery into the soil system but that advanced volcanic ash weathering can proceed in the absence of vegetation in both xeric warm sites, and cool sites depending on how old the sites are. The results indicate rainfall anywhere between 1,500 and 2,500 mm rainfall (coupled with vegetation inputs) may provide sufficient carbon delivery to saturate available C sorption sites but that less rainfall than that may result in carbon delivery being a limiting factor for C storage (depending on the degree of weathering of the volcanic ash). SRO minerals on Mauna Kea estimated at ~250–300 mm rainfall contain less carbon than either moist mesic (2,500 mm rainfall) sites in Hawaii or Mount Shasta.

Changes in soil organic matter composition on Mauna Kea

The C/N ratio of the organic matter increased from ~8 at the highest-elevation (3,560 m, ~250 mm rainfall) site to 13 at the 3,260-m-elevation site (~400 mm rainfall), and 14 at the 3,030-m-elevation (~500 mm rainfall) site, likely due to the greater influence from plants in the soil system with increasing rainfall (Table 1, Fig. 8B). The low C/N ratio of the limited soil C inputs that do occur at the driest, highest-elevation sites indicates the material is likely of microbial origin or has been highly processed by microbes. As rainfall increases

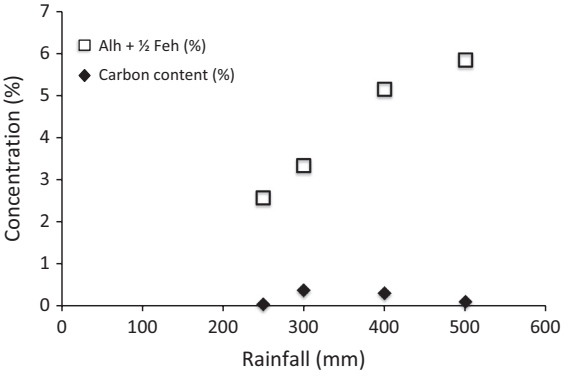

FIG. 6. Changes in rainfall in relation to carbon concentration (%) and SRO mineral abundance (as measured by Alh + 1/2 Feh) from cinder soil horizons across the climate sequence. Rainfall:C content ($P > 0.05$), rainfall:SRO content ($P < 0.05$, $r^2 = 0.48$, $n = 4$ samples).

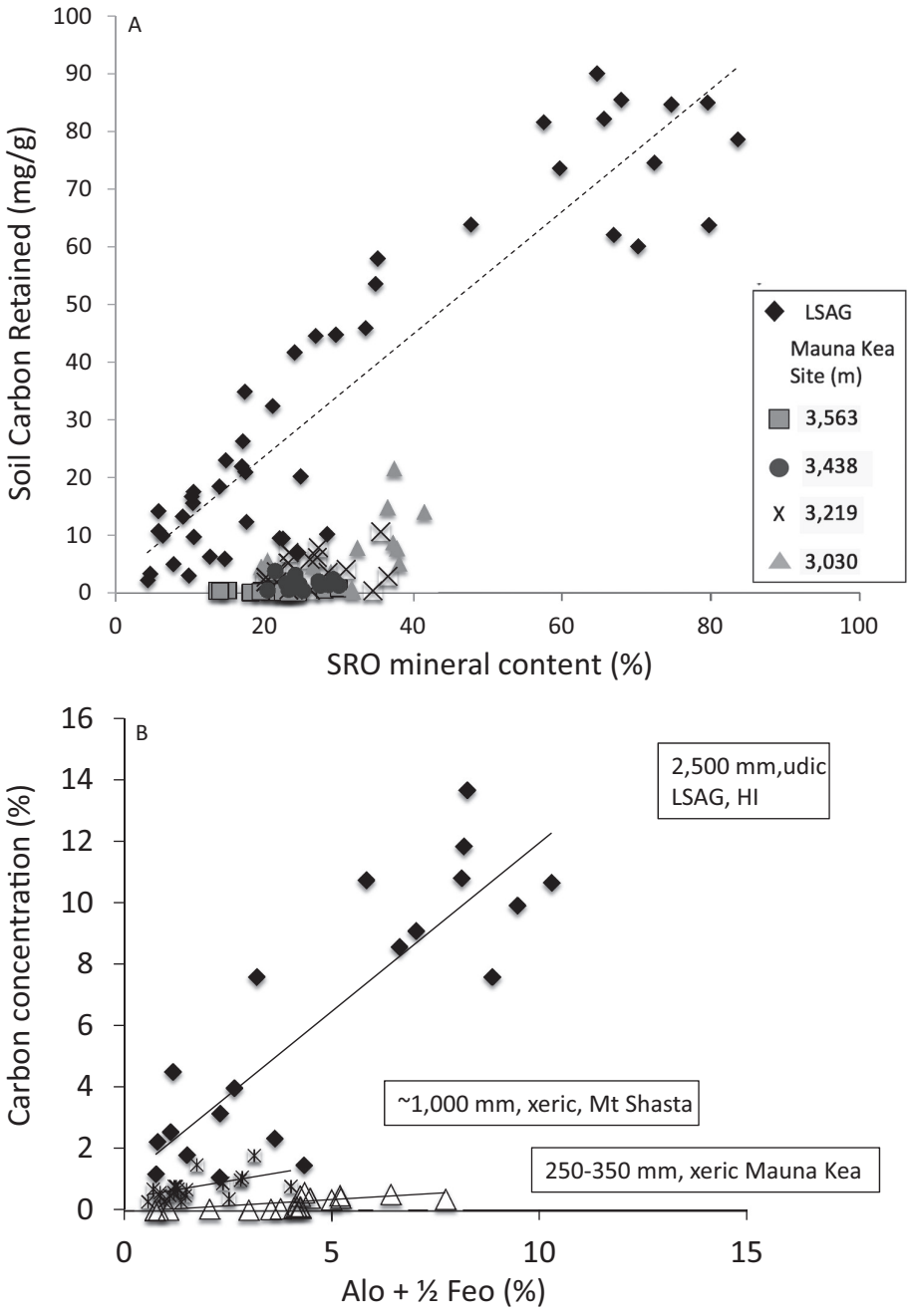

FIG. 7. (A) Quantity of C retained by SRO minerals across 2,500 mm chronosequence in Hawaii (Kramer et al. 2012; Long Substrate Age Gradient [LSAG]), and the climate gradient on Mauna Kea (this study). (B) Soil C concentration in relation to SRO minerals (as measured by selective extraction) across 2,500 mm chronosequence in Hawaii (Kramer et al. 2012), a 1,000 mm xeric site in Mount Shasta (Takahashi et al. 1993) and the ~250 mm, 300 mm rainfall sites on Mauna Kea (this study).

on Mauna Kea, the C/N ratio steadily increases, reaching a maximum of 32 at the low-elevation 2,500 mm rainfall site (Fig. 8B). Kramer et al. (2012) using NMR spectroscopy found the soil C at depth at this 20 kyr site was comprised largely of oxidized lignin, with strong chemical resemblance to dissolved organic matter (DOM) derived from overlying thick organic soil horizons. Our results show that the forms of soil carbon shift consistently across the rainfall gradient in while soil mineralogy remains relatively uniform.

As the ecosystem assemblage changes from barren desert at the summit of Mauna Kea to densely forested at

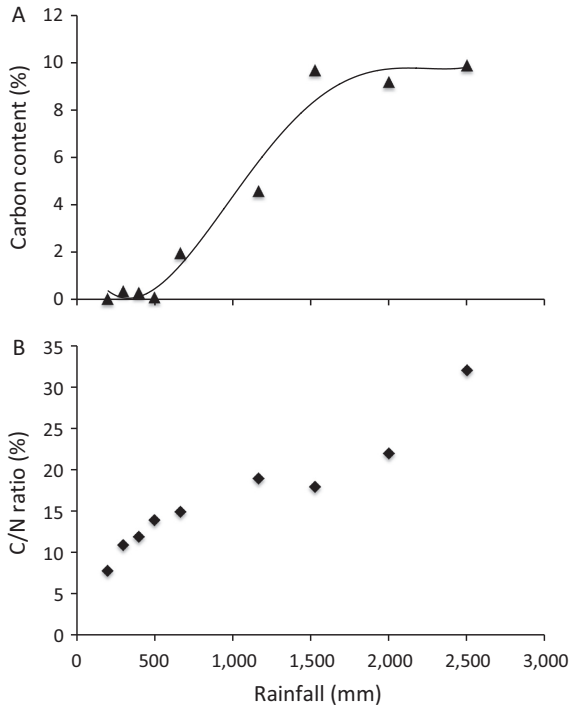

FIG. 8. (A) Soil C content (%) in deep cinder or Bw horizons in relation to rainfall across a 250–2,500 mm rainfall gradient on Mauna Kea. (B) C/N ratio in deep cinder or Bw horizons in relation to rainfall across a 250–2,500 mm rainfall gradient on Mauna Kea: ~250–500 mm (this study), 660–2,000 mm (Longathan and Swindale 1963), 2,500 mm (Kramer et al. 2012).

lower elevations, so too does the amount and chemical composition of SOM accumulation in the subsoil (Fig. 8A, B). Overall, the trend of increasing C/N ratio of subsoil C with increasing rainfall indicates the carbon accumulating at depth is increasingly of plant origin and largely comprised of oxidized lignin at sites with rainfall >1,500 mm. At these wetter sites, forested overstory and thick organic soil horizons coupled with abundant rainfall results in significant transport of DOC to depth (Kramer et al. 2012). Our results, coupled with those of Takahashi et al. 1993 and Longathan and Swindale (1963) and Kramer et al. (2012) indicate carbon transport at depth may be more limited at sites with <1,500 mm rainfall on Mauna Kea.

Changes in soil carbon composition and amount across the entire Mauna Kea climate gradient show that the rate of carbon supply to the subsoil (driven by the coupling of rainfall and aboveground plant production) determines the forms and amount of SOM accumulation. Comparison with another 1,000 mm rainfall xeric ecosystem (Takahashi et al. 1993) indicates this may be true in other ecosystems, whenever rainfall-mediated carbon supply becomes a limiting factor. Thus, while soil mineralogy may exert strong control on the amount and chemical composition of carbon accumulating in soil Kramer et al. 2012), carbon delivery is also a strong determinant of carbon composition and amount, especially at lower (<1,500 mm) rainfall.

CONCLUSIONS

Across the entire (300–4,000 m elevation, 2,500–250 mm rainfall) climate sequence we evaluated on Mauna Kea, mineralogy is relatively uniform and is dominated by SRO minerals. Thus Mauna Kea represents a unique topographic and climatic setting in which both parent material and soil mineralogy are uniform under a varying climate over a very wide elevation gradient. Most other climate gradients in Hawaii, while uniform in parent material vary in the soil mineralogy across the gradient—ranging from crystalline to short range ordered minerals depending on substrate age and rainfall in addition to retaining pedogenic carbonate (Chadwick et al. 2003, Chadwick and Chorover 2001). In part, this may be due to warmer and drier conditions and greater soil evaporation rates prevailing at low-elevation rain shadow locations, which would drive greater weathering for the same age deposits. In addition these other sites may have shown greater mineralogical differentiation because they are nearly an order of magnitude older than the Mauna Kea deposits studied here.

Our results fill an important mechanistic gap in understanding alterations of volcanic ash that can occur at high elevation during the earliest phase of soil development. After 20 kyr, the high-elevation soils of Mauna Kea have advanced in weathering such that they are capable of retaining a significant store of soil C due to the SRO minerals that have formed there. However, C accumulation in the cinder layers is notably lacking (Table 1). Plant and water inputs into the soil system were found to be the major limiting factor for soil C accumulation up to a rainfall amount of approximately 1,500 mm. Weathering processes were strongly influenced by the limiting rainfall that did occur and by the cool temperatures with the degree of alteration of the volcanic ash increased with increasing rainfall between ~250 and 500 mm rainfall. Leaching and elemental loss of mobile elements was, however, limited.

The results suggest a decoupling between weathering processes and the role of rainfall-mediated carbon delivery from plants into the soil system. Over the longer-term, our study shows that volcanic ash on Mauna Kea has been significantly altered and weathered in this high-elevation climate long before island subsidence occurs and soil development continues at lower elevation. Higher rainfall and greater influence from plants, which can occur at lower elevations, will further chemically weather the soil begin to leach Si and other mobile elements such as Ca from the soil system further lowering base saturation and increasing C storage (Fig. 8A). Eventually (with sufficient time) a shift of soil mineralogy to a more crystalline form that retains less soil carbon will occur (Vitousek 2004).

ACKNOWLEDGMENTS

We thank Heraldo Farrington for help with field logistics and sampling; Dyke Andreason at the University of California Santa Cruz (UCSC) light stable isotope facility for help determining elemental C and N; Geoff Kahl at WSU Vancouver for help conducting hydrloxlamine and oxalate extractions; and Wesley Yuen at UCSC for help with particle-size extractions.

Literature Cited

Bern, C. R., A. Thompson, and O. A. Chadwick. 2015. Quantification of colloidal and aqueous element transfer in soils: the dual-phase mass balance model. Geochimica et Cosmochimica Acta 151:1–18.

Berner, R. A. 1992. Weathering, plants, and the long-term carbon cycle. Geochimica et Cosmochimica Acta 56:3225–3231.

Blakemore, L. C., P. L. Searle, and B. K. Daly. 1987. Methods for chemical analysis of soils. New Zealand Bureau Scientific Report 80. New Zealand Soil Bureau, Lower Hutt, New Zealand.

Burt, R. 2004. Soil Survey Laboratory Methods Manual. Soil Survey Investigations Report 4, 42. USDA-NRCS, Lincoln, Nebraska, USA.

Chadwick, O. A., R. T. Gavenda, E. F. Kelly, K. Ziegler, C. G. Olson, W. C. Elliott, and D. M. Hendricks. 2003. The impact of climate on the biogeochemical functioning of volcanic soils. Chemical Geology 202:195–223.

Chadwick, O. A., and J. Chorover. 2001. The chemistry of pedogenic thresholds. Geoderma 100:321–353.

Chorover, J., M. K. Amistadi, and O. A. Chadwick. 2004. Surface charge evolution of mineral-organic complexes during pedogenesis in Hawaiian basalt. Geochimica et Cosmochimica Acta 68:4859–4876.

Cochran, F. M., and R. A. Berner. 1996. Promotion of chemical weathering by higher plants: field observations on Hawaiian basalts. Chemical Geology 132:71–77.

Dahlgren, R. A., M. Saigusa, and F. C. Ugolini. 2004. The nature, properties and management of volcanic soils. Advances in Agronomy 82:114–183.

Giambelluca, T. W., Q. Chen, A. G. Frazier, J. P. Price, Y.-L. Chen, P.-S. Chu, J. K. Eischeid, and D. M. Delparte. 2013. Online Rainfall Atlas of Hawai'i. Bulletin of the American Meteorological Society 94:313–316.

Hartt, C. E., and M. C. Neal. 1940. The plant ecology of Mauna Kea, Hawaii. Ecology 21:237–266.

Kaiser, K., and G. Guggenberger. 2000. The role of DOM sorption to mineral surfaces in the preservation of organic matter in soils. Organic Geochemistry 31:711–725.

Kettler, T. A., J. W. Doran, and T. L. Gilbert. 2001. Simplified method for soil particle-size determination to accompany soil-quality analyses. Soil Science Society of America Journal 65:849–852.

Kramer, M. G., J. Sanderman, O. A. Chadwick, J. Chorover, and P. M. Vitousek. 2012. Long-term carbon storage through retention of dissolved aromatic acids by reactive particles in soil. Global Change Biology 18:2594–2605.

Kramer, M. G., P. Sollins, R. S. Sletten, and P. K. Swart. 2003. N isotope fractionation and measures of organic matter alteration during decomposition. Ecology 84: 2021–2025.

Raine, C. T. 1939. Meteorological reports of the Mauna Kea expedition 1935 (II). The meteorological observations at Lake Waiau, August 8–19, 1935. Bulletin of the American Meteorological Society 20:97–103.

Rebecca, B. 2004. Soil survey laboratory methods manual. Soil Survey Laboratory Investigations Report 42.

Schoeneberger, P. J. et al. 1998. Field book for describing and sampling soils. Lincoln: Natural Resources Conservation Service, USDA, National Soil Survey Center.

Soil Conservation Service, USDA. 1973. Soil survey of the island of Hawaii, State of Hawaii. Soil Conservation Service in cooperation with the University of Hawaii Agricultural Experiment Station. U.S. Government Printing Office, Washington, D.C., USA.

Sollins, P., M. G. Kramer, C. Swanston, K. Lajtha, T. Filley, A. K. Aufdenkampe, … and R. D. Bowden. 2009. Sequential density fractionation across soils of contrasting mineralogy: evidence for both microbial-and mineral-controlled soil organic matter stabilization. Biogeochemistry, 96:209–231.

Takahashi, T. I., R. Dahlgren, and P. van Susteren. 1993. Clay mineralogy and chemistry of soils formed in volcanic materials in the xeric moisture regime of northern California. Geoderma 59:131–150.

Ugolini, F. C. 1974. Hydrothermal origin of the clays from the upper slopes of Mauna Kea, Hawaii. Clays and Clay Minerals 22:189–194.

Ugolini, F. C. 1975. Soils of the high elevation of Mauna Kea, Hawaii, an analogy to Martian Soils? International Colloqium Of Planetary Geology 1:531–524. Rome, Italy.

Vitousek, P. M., and O. A. Chadwick. 2013. Pedogenic thresholds and soil process domains in basalt-derived soils. Ecosystems 16:1379–1395.

Vitousek, P. M., O. A. Chadwick, T. E. Crews, J. H. Fownes, D. M. Hendricks, and D. Herbert. 1997. In this Month's issue: soil and ecosystem development across the Hawaiian Islands. GSA Today, 7:9.

Vitousek, P. M. 2004. Nutrient cycling and limitation: Hawai'i as a model system. Princeton University Press, Princeton, New Jersey, USA.

Wada, K. 1989. Allophane and imogolite. Pages 1051–1877 *in* J. B. Dixon and S. B. Weed, editors. Minerals in the soil environment. Third edition. Soil Science of America, Book Series No. 1. ASA and SSSA, Madison, Wisconsin, USA.

Wolf, E. W., and J. Morris. 1996. Geologic Map of the Island of Hawaii. U.S. Geological Survey Map I-2524-A. U.S. Geological Survey, Reston, Virginia, USA

Woodcock, A. H., M. Rubin, and R. A. Duce. 1966. Deep layer of sediments in alpine lake in the tropical mid-Pacific. Science 154:647–648.

Woodcock, A. H. 1974. Permafrost and climatology of a Hawaii volcano crater. Arctic and Alpine Research 1:49–62.

Ziegler, K., J. C. Hsieh, O. A. Chadwick, E. F. Kelly, D. M. Hendricks, and S. M. Savin. 2003. Halloysite as a kinetically controlled end product of arid-zone basalt weathering. Chemical Geology 202:461–478.